

# Entropy production from waiting-time distributions for overdamped Langevin dynamics

Ellen Meyberg, Julius Degünther, and Udo Seifert

II. Institut für Theoretische Physik, Universität Stuttgart, 70550 Stuttgart, Germany

E-mail: [meyberg@theo2.physik.uni-stuttgart.de](mailto:meyberg@theo2.physik.uni-stuttgart.de)

28 February 2024

**Abstract.** For a Markovian dynamics on discrete states, the logarithmic ratio of waiting-time distributions between two successive, instantaneous transitions in forward and backward direction is a measure of time-irreversibility. It thus serves as an entropy estimator, which is exact in the case of a uni-cyclic network. We adopt this framework to overdamped Langevin dynamics, where such transitions have finite duration. By introducing milestones based on the observation of a particle at at least three points, we identify an entropy estimator that becomes exact for driven motion along a one-dimensional potential.

*Keywords:* Entropy estimator, waiting-time distribution, coarse-graining

Submitted to: *J. Phys. A: Math. Theor.*

*Introduction and Motivation.*— Estimating entropy production from coarse-grained data is a challenging problem in thermodynamic inference [1]. Recently, waiting-time distributions have been identified as an efficient tool for models with an underlying Markovian dynamics on a network of discrete states [2–5]. These estimators complement other inequalities, such as [6–14], that also provide lower bounds on quantifying irreversibility. Entropy estimators based on waiting-time statistics between few observable transitions in a Markov network have gained particular interest [15, 16]. There, the time-reversal asymmetry is encoded in the difference between the waiting-time distributions of two successive forward and backward transitions. Surprisingly, these estimators recover the full entropy production rate in a uni-cyclic system with a single observed transition. More generally, the waiting-time approach can be applied to any observations of Markovian events [17], not only to transitions.

Whether and how these concepts can be applied to systems with an underlying continuous dynamics, like an overdamped Langevin dynamics, seems to have been explored less extensively yet. One route is to lump the continuous states into discrete ones [18–20] using for example Kramer’s rates [21]. However, except for limiting cases, state-lumping yields an effective non-Markovian dynamics, which typically prevents recovering the full entropy production [22]. Alternatively, state-like events for overdamped Langevin dynamics can be defined through milestones [23, 24]. The milestone scheme relies, in the case of one-dimensional motion, on the identification of certain points as states that characterize the state of the system as long as no other such state is visited. It has been shown that this type of coarse-graining preserves the affinity of a cycle [23]. Although that study provides us with a definition of a state-like event that resembles a Markov state in discrete networks, it lacks a definition of a transition between those.

In this work, we first explain how transitions can be defined for one-dimensional, overdamped Langevin dynamics based on milestone. In a second step, we prove that the associated affinity and entropy estimators inspired by [15] are exact. We demonstrate that, in order to measure the affinity of a cycle, an experimentalist needs to observe at least three points on it.

*Model.*— We consider one-dimensional overdamped Langevin dynamics of a particle on a ring of length  $L$  in a periodic, time-independent potential  $V(x)$  under the influence of a driving force  $f$  described by

$$\dot{x}(t) = \mu F(x) + \xi(t) = \mu[-\partial_x V(x) + f] + \xi(t). \quad (1)$$

Here  $\mu$  denotes the mobility, the thermal energy  $k_B T$  is set to unity and the random force obeys

$$\langle \xi(t) \rangle = 0 \quad \text{and} \quad \langle \xi(t') \xi(t) \rangle = 2\mu \delta(t - t'). \quad (2)$$

Equivalently, the dynamics can be described with the Fokker-Planck equation

$$\partial_t p(x, t) = -\partial_x j(x, t) = -\mu \partial_x [F(x) - \partial_x] p(x, t), \quad (3)$$

which describes the evolution of the probability density  $p(x, t)$  with periodic boundary conditions. In the steady state, i.e., for  $\partial_t p^s(x) = 0$ , a constant stationary current  $j^s$

develops. The driving affinity, i.e., the entropy production per cycle, is given by

$$\mathcal{A} = fL \quad (4)$$

independently of  $V(x)$  leading to the entropy production rate in the stationary state

$$\sigma = j^s \mathcal{A}. \quad (5)$$

For a uni-cyclic, discrete network as shown in figure 1 a) the affinity is given by

$$\mathcal{A} = \sum_{(mn)} \ln \left( \frac{k_{mn}}{k_{nm}} \right), \quad (6)$$

where the transition rates  $k_{mn}$  and  $k_{nm}$  connect two neighbouring states  $m$  and  $n$ . The summation includes all edges  $(mn)$  of the cycle. It has been shown in [15] that  $\mathcal{A}$  can be inferred from waiting time distributions

$$\psi_{I \rightarrow J}(\tau) \equiv P(J, \tau | I, 0), \quad (7)$$

which is the probability for transition  $J$  to happen after a time  $\tau$  given the previous transition  $I$ . To be specific, we consider the pair of transitions between states  $a$  and  $b$  called  $I_+$  and  $I_-$  in figure 1 a). The logarithmic ratio of waiting-time distributions

$$\hat{\mathcal{A}}(\tau) \equiv \ln \left( \frac{\psi_{I_+ \rightarrow I_+}(\tau)}{\psi_{I_- \rightarrow I_-}(\tau)} \right) \quad (8)$$

between two successive transitions in clockwise,  $I_+ \rightarrow I_+$ , and anti clockwise direction,  $I_- \rightarrow I_-$ , serves as time-independent and exact estimator of the affinity  $\mathcal{A}$ . The proof of this relation crucially depends on the Markovianity of the dynamics [15]. Our goal is to find an equivalent procedure for continuous states as required for the particle on a ring.

First of all, we need to identify transitions, whose crucial property is to resolve the particle's direction of motion [22]. Furthermore, if we can observe only one pair of transitions, two successive ones in the same direction should be equal to a full passage of the cycle. Since the velocity for overdamped dynamics is not well defined, a definition of a transition based on the directed crossing of a milestone, i.e., a fixed position on the ring, is not possible.

We, therefore, have to introduce two milestones  $A$  and  $B$  through two points with  $x$ -coordinates

$$A \equiv (x = x_A \bmod L) \quad \text{and} \quad B \equiv (x = x_B \bmod L) \quad (9)$$

with periodic boundary conditions as illustrated in figure 1 b). Without loss of generality,  $x_A$  can be set to zero. If we apply the milestoning scheme as coarse-graining, an effective trajectory thus becomes binary. It is either in state  $A$  or  $B$  depending on whether the position  $x_A$  or  $x_B$  was visited latest, respectively. Transitions  $I_{\pm}$  are identified as passages in opposite direction between the two milestones,

$$I_+ \equiv A \xrightarrow{C} B \quad \text{and} \quad I_- \equiv B \xrightarrow{C} A, \quad (10)$$

where  $C$  on top of the arrow denotes an auxiliary, third point. The latter ensures that a transition corresponds to the passage along the shorter route between  $A$  and

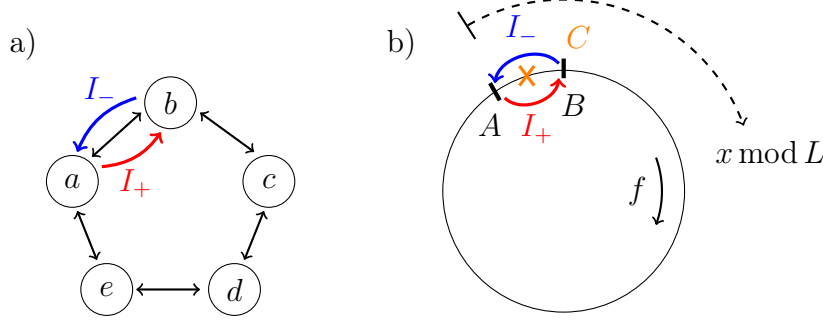


**Figure 1.** Illustration of the analogy between transitions in discrete and continuous one-dimensional stochastic systems. a) Discrete five-state ring with transitions  $I_{\pm}$  between states  $a$  and  $b$ , black arrows denote that two states are connected. b) Continuous ring of length  $L$  with driving force  $f$  and milestones  $A$  and  $B$ , the  $(x \bmod L)$ -coordinate of state  $A$  is arbitrarily set to zero. Observing the additional state  $C$  marked with a cross allows to distinguish clockwise and counter clockwise motion between  $A$  and  $B$ .

$B$ , as illustrated in figure 1 b). This implies that inference based on waiting times for overdamped Langevin dynamics requires a set of at least three observed points. A transition  $I_+$  and  $I_-$  ends if endpoints  $B$  and  $A$ , respectively, are reached. Crucially, the state of the system is fully characterized each time a transition is finished, because reaching a milestone  $A$  or  $B$  is a Markovian event [17]. In contrast to transitions between discrete states, the continuous ones possess a finite duration, which ends when the milestone is reached.

In the discrete case, waiting-time distributions can be determined from solving the absorbing master equation [15, 25], where the observed links lead to states that the particle cannot leave, i.e., to absorbing states, as shown in figure 2 a). Analogously, in the present continuous case, we have to consider an interval  $0 \leq x \leq L + x_B$ , as illustrated in figure 2 b), and to solve the Fokker-Planck equation (3) with absorbing boundary conditions that read [26, 27]

$$p(x = 0, \tau) = 0 \quad \text{and} \quad p(x = L + x_B, \tau) = 0. \quad (11)$$

Waiting-time distributions are thus equal to the fluxes through absorbing boundaries at  $A'$  and  $B$  given the initial position as fixed by the position after the last transition, here set to  $\tau = 0$ . This leads to

$$\psi_{I_+ \rightarrow I_+}(\tau) = j(L + x_B, \tau | x_B, 0), \quad (12a)$$

$$\psi_{I_- \rightarrow I_-}(\tau) = -j(0, \tau | L, 0), \quad (12b)$$

$$\psi_{I_+ \rightarrow I_-}(\tau) = -j(0, \tau | x_B, 0), \quad (12c)$$

$$\psi_{I_- \rightarrow I_+}(\tau) = j(L + x_B, \tau | L, 0), \quad (12d)$$

where the signs are chosen so that the waiting-time distributions are positive. We have conditioned the fluxes on the initial position  $x = x_B$  after  $I_+$  and  $x = L$  after  $I_-$ , respectively.

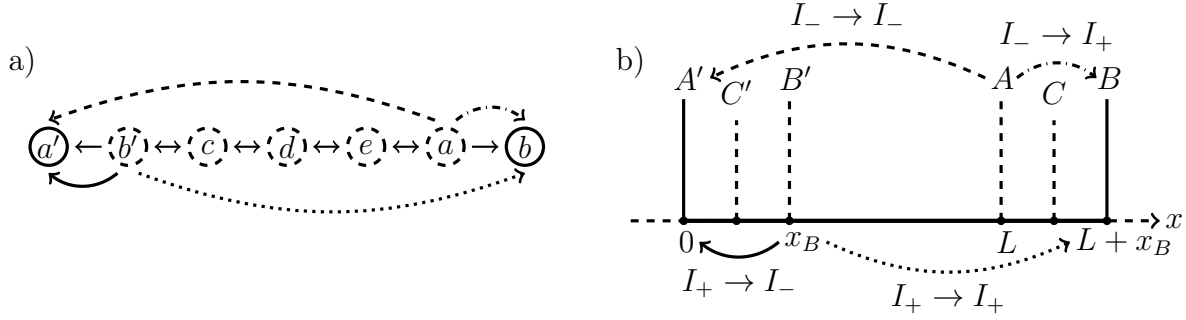


**Figure 2.** System with absorbing states. a) Discrete network with absorbing states  $a'$  and  $b$  marked with full circles, otherwise dashed. b) Full vertical lines denote absorbing boundaries placed at milestones  $A'$  and  $B$ . The states  $A, A', B, B'$  and  $C, C'$  are equivalent points on the ring mod  $L$  where we have set  $x_A = 0$ . The precise location of  $C$  between  $A$  and  $B$  is arbitrary.

*Entropy estimator.*— After identifying waiting-time distributions for continuous stochastic systems we now want to apply the estimator (8). Without any driving force  $f$ , i.e. in equilibrium, the cycle is equally likely passed in both directions. However, for non-vanishing  $f$  in clockwise-direction, two subsequent  $I_+$  transitions get more likely than two  $I_-$  ones. Hence, we expect that  $\hat{\mathcal{A}}(\tau)$  measures time-irreversibility and is related to the affinity  $\mathcal{A}$  of a cycle similar to the discrete case. In fact, we will show that

$$\hat{\mathcal{A}}(\tau) = \mathcal{A} = fL. \quad (13)$$

On a theoretical level, waiting-time distributions can also be understood as

$$\psi_{I \rightarrow J}(\tau) = \sum_{\zeta \in \{\zeta_{I \rightarrow J}^\tau\}} \mathcal{P}[\zeta|I] = \sum_{\zeta \in \{\zeta_{I \rightarrow J}^\tau\}} \mathcal{P}[\zeta|X_I], \quad (14)$$

i.e., as the sum over all path-weights  $\mathcal{P}$  of trajectories  $\zeta_{I \rightarrow J}^\tau$  that start at the endpoint of transition  $I$  and that end at the one of  $J$  after time  $\tau$  without undergoing any other transitions in between. The conditioning on the first transition  $I$  in (14) can be replaced by a conditioning on the milestone  $X_I \in \{A, B\}$  at the end of this snippet. In the following, we will call microscopic paths connecting two transitions snippets.

We assume that we cannot observe the full trajectory  $\gamma = x(t)$  but only transitions  $I_+$  and  $I_-$ . The effective trajectory  $\Gamma$  equals a sequence of such transitions after certain waiting-times  $\tau_i$ . Therefore, the information gained through the measurement can be represented by tuples  $(I_\pm, \tau_i)$ . For the section of trajectory shown in figure 3, we get

$$\Gamma = \dots \rightarrow (I_-, \tau_0) \rightarrow (I_+, \tau_1) \rightarrow (I_+, \tau_2) \rightarrow (I_-, \tau_3) \rightarrow \dots. \quad (15)$$

Such data retains all available information and thus suffice to evaluate the waiting-time distributions (7). The coarse-grained sequence  $\Gamma$  can be realized on the microscopic level by many different trajectories  $\gamma$ , e.g., by

$$\gamma = \dots \rightarrow \zeta_{I_- \rightarrow I_+}^{\tau_1} \rightarrow \zeta_{I_+ \rightarrow I_+}^{\tau_2} \rightarrow \zeta_{I_+ \rightarrow I_-}^{\tau_3} \rightarrow \dots, \quad (16)$$

that consist of snippets  $\zeta_{I \rightarrow J}^\tau$  of length  $\tau$  connecting two transitions  $I$  and  $J$ . All contributing  $\gamma$  share the same sequence of transitions and associated duration, i.e.,

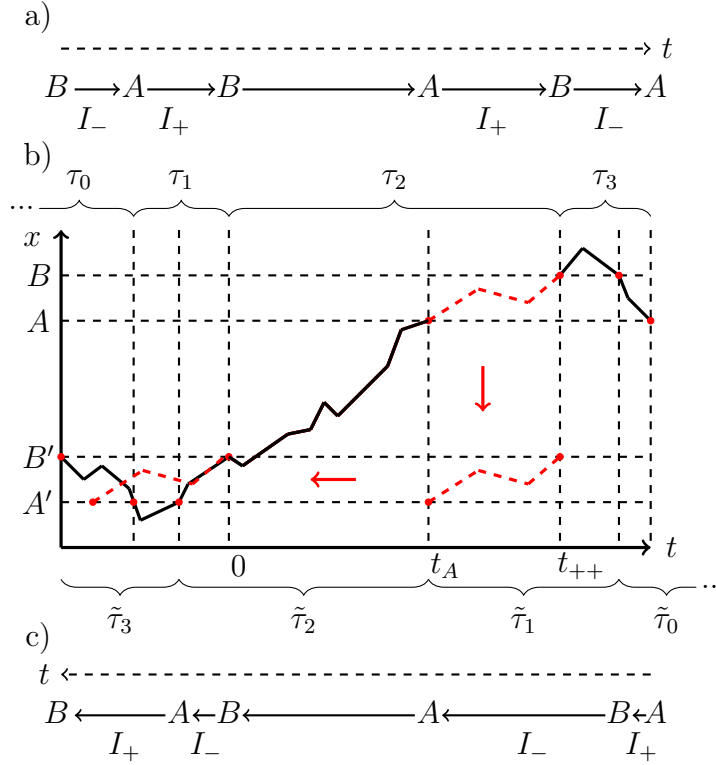


**Figure 3.** Illustration of trajectories and time-reversal. a) Coarse-grained two-state trajectory with sequence of transitions. b) Corresponding schematic Langevin trajectory divided into snippets between transitions. Their duration  $\tau_i$  is indicated by curly brackets. The bijective mapping between  $\mathcal{R}(\zeta_{I_+ \rightarrow I_+}^\tau)$  and  $\zeta_{I_- \rightarrow I_-}^\tau$  is possible by translating the dashed part of the trajectory in time. The starting point of the snippet of length  $\tau_2$  is arbitrarily set to  $t = 0$ . c) Time-reversed coarse-grained trajectory and sequence of transitions. The time-reversal changes the times at which the transitions are recorded as well as the duration of the snippets.

the tuples in (15). We can express  $\mathcal{P}[\Gamma]$  using the Markov property of transitions and sum over all snippets connecting the respective transitions to arrive at

$$\mathcal{P}[\Gamma] = \dots \sum_{\zeta \in \{\zeta_{I_- \rightarrow I_+}^{\tau_1}\}} \mathcal{P}[\zeta|A'] \sum_{\zeta \in \{\zeta_{I_+ \rightarrow I_+}^{\tau_2}\}} \mathcal{P}[\zeta|B'] \sum_{\zeta \in \{\zeta_{I_+ \rightarrow I_-}^{\tau_3}\}} \mathcal{P}[\zeta|B] \dots \quad (17)$$

for the example shown in figure 3 b). Since the sums equal the waiting-times in (14), the path weight (17) becomes

$$\mathcal{P}[\Gamma] = \dots \psi_{I_- \rightarrow I_+}(\tau_1) \psi_{I_+ \rightarrow I_+}(\tau_2) \psi_{I_+ \rightarrow I_-}(\tau_3) \dots \quad (18)$$

From the trajectory shown in figure 3 it should be clear that, while all paths contributing to  $\psi_{I_\pm \rightarrow I_\pm}(\tau)$  form closed loops, the ones contributing to  $\psi_{I_\pm \rightarrow I_\mp}(\tau)$  do not because the latter begin and end at different milestones.

To compute the entropy produced by  $\Gamma$ , its time-reversed version

$$\tilde{\Gamma} = \dots \rightarrow (I_+, \tilde{\tau}_0) \rightarrow (I_-, \tilde{\tau}_1) \rightarrow (I_-, \tilde{\tau}_2) \rightarrow (I_+, \tilde{\tau}_3) \rightarrow \dots, \quad (19)$$

is needed, for which we replace every  $I_+$  transition with an  $I_-$  transition and vice versa in the sequence (15). In the time-reversed trajectory as shown in figure 3c), these transitions occur at different times, since they possess a finite duration. Hence, also the duration  $\tau_i$  of a snippet changes to  $\tilde{\tau}_i$  under time-reversal. Coarse-graining the time-reversed trajectory at the state-level thus leads to a phenomenon called kinetic hysteresis described in [23], i.e., in this setup, time reversal and coarse-graining do not commute. Additionally, at the transition level, the duration of the snippets change and the transitions are measured at different absolute times. The time-reversed version of a trajectory that undergoes two subsequent  $I_+$  transitions will undergo two subsequent  $I_-$  ones. However, the waiting-time gets altered, i.e., in the example  $\tau_2 \neq \tilde{\tau}_2$ . In the forward trajectory the  $I_+$  transition is finished at  $t_{++} = \tau_2$  after a preceding  $I_+$  one, see the time axis. If we reverse the trajectory in time, this part of the trajectory does not correspond to a  $I_- \rightarrow I_-$  sequence.

Thus, in order to compare the effect of time-reversal on the microscopic and on the coarse-grained level, we have to compare how the trajectories and waiting-time distributions are modified. Since it is known how the time-reversal operation  $\mathcal{R}$  acts on the microscopic level, i.e. on trajectories  $\gamma$  and snippets  $\zeta_{I \rightarrow J}^\tau$ , we can investigate whether every time-reversed snippet connecting two  $I_+$  transitions can be mapped to a snippet with equal path weight connecting two  $I_-$  transitions in the original dynamics, i.e.,

$$\mathcal{P}[\mathcal{R}(\zeta_{I_+ \rightarrow I_+}^\tau) | \tilde{I}_+] = \mathcal{P}[\zeta_{I_- \rightarrow I_-}^\tau | I_-] \quad (20)$$

holds true. In fact, this is possible and can be shown by rearranging every time-reversed  $\zeta_{I_+ \rightarrow I_+}^\tau$  trajectory using the time-translational invariance of the path weight as illustrated in figure 3b). Consider the trajectory starting at  $t = 0$  and ending at  $t_{++}$ . The time-reversed version of it starts at  $B$  and ends in  $B'$ . If we cut the dashed part, it does not matter whether we place it between  $B'$  and  $A'$  or between  $B$  and  $A$  because the states are physically equivalent and merely differ by  $L$ . In addition, the dashed path can be translated in time and thus added at the end of the time-reversed trajectory at state  $B'$ . This leads to a modified trajectory that equals a snippet connecting two  $I_-$  transitions thus confirming (20). The length of the original snippet and the modified one coincide and they both complete the cycle once. As a consequence,

$$\psi_{\tilde{I}_+ \rightarrow \tilde{I}_+}(\tau) = \sum_{\zeta \in \{\zeta_{I_+ \rightarrow I_+}^\tau\}} \mathcal{P}[\mathcal{R}(\zeta) | \tilde{I}_+] = \psi_{I_- \rightarrow I_-}(\tau) \quad (21)$$

holds. The ratio of path weights between the two snippets that complete the cycle once in opposite direction obeys

$$\frac{\mathcal{P}[\zeta_{I_+ \rightarrow I_+}^\tau | I_+]}{\mathcal{P}[\zeta_{I_- \rightarrow I_-}^\tau | I_-]} = \exp \left[ \int_0^\tau F(x(t)) \dot{x}(t) dt \right] = e^{fL} = e^{\mathcal{A}} \quad (22)$$

similar to [28]. Multiplying by the denominator of the left-hand side and summing over all snippets leads to

$$\psi_{I_+ \rightarrow I_+}(\tau) = e^{\mathcal{A}} \psi_{I_- \rightarrow I_-}(\tau), \quad (23)$$

which implies that the estimator (8) is time-independent and that it yields the full affinity, just as the estimator for discrete dynamics does [15].

In addition, we are now able to state a relation that only uses waiting-time statistics to infer the total entropy  $\Delta S[\gamma]$  along a microscopic trajectory  $\gamma$  and its mean rate  $\sigma$ . In terms of the path weight  $\mathcal{P}[\gamma|x_i]$ , the total entropy production along  $\gamma$  is given by

$$\Delta S[\gamma] = \ln \left( \frac{\mathcal{P}[\gamma|x_i] p^s(x_i)}{\mathcal{P}[\tilde{\gamma}|x_f] p^s(x_f)} \right) \quad (24)$$

in the stationary state. Here the distribution of the initial points  $x_i$  and  $x_f$  of  $\gamma$  and  $\tilde{\gamma}$ , respectively, are taken from the steady state distribution  $p^s(x)$ . In the long-time limit, the contribution from the initial conditions becomes neglectable. The entropy produced by one trajectory  $\gamma$  can be calculated as the sum of log-ratios between probabilities of snippets. With (22) we can replace the entropy produced by closed loops by (8). Hence, it suffices to count the times  $N_{I_{\pm}}(t)$  two successive  $I_+$  and  $I_-$  transitions are observed on the coarse-grained level up to time  $t$  to arrive at

$$\Delta S[\gamma] = (N_{I_+ \rightarrow I_+}(t) - N_{I_- \rightarrow I_-}(t)) \ln \left( \frac{\psi_{I_+ \rightarrow I_+}(t)}{\psi_{I_- \rightarrow I_-}(t)} \right). \quad (25)$$

Thus, waiting-time statistics can be used to infer the whole distribution of entropy production. In the long-time-limit  $I_{\pm} \rightarrow I_{\mp}$  do not contribute, since  $N_{I_+ \rightarrow I_-}(t) - N_{I_- \rightarrow I_+}(t)$  is equal to  $0, \pm 1$ . The mean entropy production rate  $\sigma$  then follows from (5) with

$$j^s = \lim_{t \rightarrow \infty} \frac{N_{I_+ \rightarrow I_+}(t) - N_{I_- \rightarrow I_-}(t)}{t}. \quad (26)$$

*Summarizing perspective.*— We have identified a Markovian event for one-dimensional, overdamped Langevin dynamics that can be used to infer the affinity in a uni-cyclic system by analyzing waiting-times between successive events. Transitions correspond to passages between two milestones with a certain orientation that is detected using an auxiliary state in between. Just like for discrete dynamics, the key property of events that here yield an exact estimator is Markovianity [17]. Furthermore, we obtain the distribution of entropy production from waiting-time distributions.

The presented formalism can easily be applied to arbitrary graphs consisting of connected, one-dimensional continuous paths like the ones described in [23]. If we define transitions as passages between nodes of the network in the same manner as for the uni-cyclic system, the results obtained in [15] for multi-cyclic discrete systems hold true. To be specific, the estimator (5) then becomes time-dependent and is bounded by the smallest affinity and the largest one of all cycles that contain the observed transition. Moreover, our approach simplifies the theoretic framework used in [23] because only the Markovian property of the milestones is required to adapt the proofs based on snippets. It further underlines that milestoneing always bounds the entropy production if reaching the milestone is a Markovian event [17].

In principle, this approach is not limited to one-dimensional systems. For a two-dimensional one like a particle driven along a torus it would be interesting to exploit the



definition of transitions between milestones that in this setup could correspond to closed curves that cannot be contracted to a point. However, since the Markov property only applies to points and not to curves, hitting a curve is a non-Markovian event. Thus, the discussion from [17] applies and we expect that the estimator (8) does not yield a bound on the full entropy production.

Another open question is the application to underdamped Langevin dynamics for which the distinction between forward and backward transitions does not require the auxiliary point  $C$  if positive and negative velocities at one single milestone could be discerned. However, without access to the precise value of the velocity, registering such an event is still non-Markovian [29], which means that a bound on entropy production cannot be expected, in general.

## Acknowledgments

We thank Jann van der Meer for stimulating discussions.

## References

- [1] Udo Seifert. From Stochastic Thermodynamics to Thermodynamic Inference. *Annual Review of Condensed Matter Physics*, 10:171–192, 2019.
- [2] Ignacio A Martínez, Gili Bisker, Jordan M Horowitz, and Juan MR Parrondo. Inferring broken detailed balance in the absence of observable currents. *Nature communications*, 10:3542, 2019.
- [3] Dominic J. Skinner and Jörn Dunkel. Estimating Entropy Production from Waiting Time Distributions. *Physical Review Letters*, 127:198101, 2021.
- [4] Jannik Ehrich. Tightest bound on hidden entropy production from partially observed dynamics. *Journal of Statistical Mechanics: Theory and Experiment*, 2021:083214, 2021.
- [5] Eden Nitzan, Aishani Ghosal, and Gili Bisker. Universal bounds on entropy production inferred from observed statistics, 2022. arXiv:2212.01783 [cond-mat].
- [6] Andre C. Barato and Udo Seifert. Thermodynamic Uncertainty Relation for Biomolecular Processes. *Physical Review Letters*, 114:158101, 2015.
- [7] Todd R. Gingrich, Jordan M. Horowitz, Nikolay Perunov, and Jeremy L. England. Dissipation bounds all steady-state current fluctuations. *Physical Review Letters*, 116:120601, 2016.
- [8] Matteo Polettini and Massimiliano Esposito. Effective Thermodynamics for a Marginal Observer. *Physical Review Letters*, 119:240601, 2017.
- [9] Izaak Neri, Édgar Roldán, and Frank Jülicher. Statistics of infima and stopping times of entropy production and applications to active molecular processes. *Physical Review X*, 7:011019, 2017.
- [10] Naoto Shiraishi, Ken Funo, and Keiji Saito. Speed limit for classical stochastic processes. *Physical Review Letters*, 121:070601, 2018.
- [11] Patrick Pietzonka and Francesco Coghi. Thermodynamic cost for precision of general counting observables, 2023. arXiv:2305.15392 [cond-mat].
- [12] Shiling Liang and Simone Pigolotti. Thermodynamic bounds on time-reversal asymmetry. *Physical Review E*, 108:L062101, 2023.
- [13] Naruo Ohga, Sosuke Ito, and Artemy Kolchinsky. Thermodynamic bound on the asymmetry of cross-correlations. *Physical Review Letters*, 131:077101, 2023.
- [14] Andreas Dechant, Jérôme Garnier-Brun, and Shin-ichi Sasa. Thermodynamic bounds on correlation times. *Physical Review Letters*, 131:167101, 2023.
- [15] Jann van der Meer, Benjamin Ertel, and Udo Seifert. Thermodynamic Inference in Partially

- Accessible Markov Networks: A Unifying Perspective from Transition-Based Waiting Time Distributions. *Physical Review X*, 12:031025, 2022.
- [16] Pedro E. Harunari, Annwasha Dutta, Matteo Polettini, and Édgar Roldán. What to learn from a few visible transitions' statistics? *Physical Review X*, 12:041026, 2022.
- [17] Jann van der Meer, Julius Degünther, and Udo Seifert. Time-Resolved Statistics of Snippets as General Framework for Model-Free Entropy Estimators. *Physical Review Letters*, 130:257101, 2023.
- [18] Robert Gernert, Clive Emary, and Sabine H. L. Klapp. On the waiting time distribution for continuous stochastic systems. *Physical Review E*, 90:062115, 2014.
- [19] Gianmaria Falasco and Massimiliano Esposito. Local detailed balance across scales: From diffusions to jump processes and beyond. *Physical Review E*, 103:042114, 2021.
- [20] Aishani Ghosal and Gili Bisker. Inferring entropy production rate from partially observed Langevin dynamics under coarse-graining. *Physical Chemistry Chemical Physics*, 24:24021–24031, 2022.
- [21] Peter Hänggi, Peter Talkner, and Michal Borkovec. Reaction-rate theory: fifty years after kramers. *Reviews of Modern Physics*, 62:251–341, 1990.
- [22] Aljaž Godec and Dmitrii E. Makarov. Challenges in Inferring the Directionality of Active Molecular Processes from Single-Molecule Fluorescence Resonance Energy Transfer Trajectories. *The Journal of Physical Chemistry Letters*, 14:49–56, 2023.
- [23] David Hartich and Aljaž Godec. Emergent Memory and Kinetic Hysteresis in Strongly Driven Networks. *Physical Review X*, 11:041047, 2021.
- [24] David Hartich and Aljaž Godec. Violation of local detailed balance upon lumping despite a clear timescale separation. *Physical Review Research*, 5:L032017, 2023.
- [25] Ken Sekimoto. Derivation of the first passage time distribution for markovian process on discrete network, 2022.
- [26] Hannes Risken. *The Fokker-Planck Equation: Methods of Solution and Applications*, volume 18 of *Springer Series in Synergetics*. Springer, Berlin, Heidelberg, 1996.
- [27] Narendra S Goel and Nira Richter-Dyn. *Stochastic models in biology*. Elsevier, 2013.
- [28] Alexander M. Berezhkovskii, Gerhard Hummer, and Sergey M. Bezrukov. Identity of Distributions of Direct Uphill and Downhill Translocation Times for Particles Traversing Membrane Channels. *Physical Review Letters*, 97:020601, 2006.
- [29] Julius Degünther, Jann van der Meer, and Udo Seifert. Fluctuating entropy production on the coarse-grained level: Inference and localization of irreversibility, 2023. arXiv:2309.07665 [cond-mat].